Katanin inhibition prevents the redistribution of γ-tubulin at mitosis

Dan Buster, Karen McNally and Francis J. McNally*

Section of Molecular and Cellular Biology, University of California, Davis, CA 95616, USA

*Author for correspondence (e-mail: fjmcnally@ucdavis.edu)

Accepted 25 November 2001

Journal of Cell Science 115, 1083-1092 (2002) © The Company of Biologists Ltd

Summary

Katanin is a microtubule-severing protein that is concentrated at mitotic spindle poles but katanin's function in the mitotic spindle has not been previously reported. Inhibition of katanin with either of two dominant-negative proteins or a subunit-specific antibody prevented the redistribution of γ-tubulin from the centrosome to the spindle in prometaphase CV-1 cells as assayed by immunofluorescence microscopy. Because γ-tubulin complexes can bind to pre-existing microtubule minus ends, these results could be explained by a model in which the broad distribution of γ-tubulin in the mitotic spindle is in part due to cytosolic γ-tubulin ring complexes binding to microtubule minus ends generated by katanin-mediated microtubule severing. Because microtubules depolymerize at their ends, we hypothesized that a greater number of microtubule ends generated by severing in the spindle would result in an increased rate of spindle disassembly when polymerization is blocked with nocodazole. Indeed, katanin inhibition slowed the rate of spindle microtubule disassembly in the presence of nocodazole. However, katanin inhibition did not affect the rate of exchange between polymerized and unpolymerized tubulin as assayed by fluorescence recovery after photobleaching. These results support a model in which katanin activity regulates the number of microtubule ends in the spindle.

Key words: Katanin, Microtubule, Mitosis, Centrosome, γ-Tubulin

Introduction

During eukaryotic cell division, chromosome segregation is mediated by a microtubule-based spindle. Spindles are assembled by at least two pathways: a centrosome-based pathway common in animal cell mitosis and an acentrosomal pathway common in female meiosis (Waters and Salmon, 1997). In both cases, microtubules are thought to be nucleated from γ-tubulin ring complexes (γ-TuRCs) (Zheng et al., 1995). In the first case, microtubules are nucleated from γ-TuRCs that are attached to the pericentriolar material of centrosomes (Moritz et al., 1998). In the second case, chromatin-associated RCC1 may create a localized concentration of GTP-Ran around chromosomes (Carazo-Salas et al., 1999), stimulating microtubule assembly through importin-β and downstream effectors (Wiese et al., 2001; Nachury et al., 2001). γ-TuRCs appear to be used even for this centrosome-independent nucleation (Wilde and Zheng, 1999).

Microtubules that have been nucleated from γ-TuRCs in vitro have minus ends that are physically capped. These γ-TuRC caps prevent minus-end polymerization and depolymerization (Wiese and Zheng, 2000; Keating and Borisy, 2000). However, two types of experimental data indicate that microtubule minus ends do depolymerize in vivo. First, minus end depolymerization has been directly observed on single microtubules in cytoplasts (Rodionov and Borisy, 1997). Second, the poleward flux of tubulin polymer in mitotic spindles (Mitchison, 1989), indicates that microtubule minus ends are constantly depolymerizing during mitosis. This minus end depolymerization in the spindle pole may provide one of several forces to drive anaphase A chromosome segregation.

If the functional minus-end capping by γ-TuRCs observed in vitro (Wiese and Zheng, 2000) is applicable in vivo, then only three mechanisms can explain microtubule minus-end depolymerization in vivo. First, some microtubules may nucleate in the cytoplasm without γ-TuRCs. Second, γ-TuRCs might detach from microtubule minus ends either due to a spontaneous exchange rate or due to a γ-TuRC uncapping enzyme. Third, a pre-existing microtubule that is broken or severed should have an exposed minus end that is at least transiently free to depolymerize. Breakage or severing of microtubules in interphase cells has been clearly documented (Waterman-Storer and Salmon, 1997; Odde et al., 1999), whereas microtubule severing in spindles cannot be directly observed due to the resolution limit of light microscopy.

Katanin has an in vitro microtubule-severing activity (McNally and Vale, 1993) and is concentrated at mitotic spindle poles in vertebrates and echinoderms (McNally et al., 1996; McNally and Thomas, 1998). Thus katanin might sever microtubules from their γ-TuRC caps and allow minus-end depolymerization during mitosis. Because γ-TuRCs cap pre-existing minus ends in vitro, it is possible that the broad microtubule-dependent distribution of γ-tubulin in vertebrate spindles (Lajoie-Mazenc et al., 1994) is partly due to cytosolic γ-TuRCs binding to severed minus ends. Two lines of evidence are consistent with this model. First, analysis of vertebrate mitotic spindles by serial EM reconstruction reveals that the minus ends of many microtubules are found at some distance from the centrosome (Mastronarde et al., 1993). Second, release of microtubules from mitotic centrosomes has been

directly observed in vitro (Belmont et al., 1990) and in vivo (Rusan et al., 2001).

Testing the hypothesis that katanin severs microtubules from their centrosomal nucleation sites during mitosis requires appropriate inhibitory reagents. Katanin is a heterodimer composed of a catalytic 60 kDa AAA subunit (p60) and an 80 kDa subunit (p80) involved in subcellular targeting (Hartman et al., 1998). We have previously demonstrated that transient expression of the C-terminal domain of the p80 katanin subunit causes dissociation of endogenous p60 subunits from mitotic spindle poles (McNally et al., 2000). We have also previously reported an affinity purified anti-p60 katanin antibody that is monospecific in cultured vertebrate cell lines and which inhibits the microtubule-severing activity present in *Xenopus* egg extracts (McNally and Thomas, 1998). Because katanin is an AAA enzyme and because point mutants of other AAA enzymes that cannot hydrolyze ATP act as dominant inhibitors of the wild-type enzyme (Babst et al., 1998), we have also developed a point mutant of p60 katanin that inhibits wild-type p60 (see below). These three inhibitors of katanin activity and localization were used in this study to investigate the role of microtubule severing at mitotic spindle poles.

Materials and Methods

Protein expression and purification

Baculoviruses expressing 6-his-wt-human p60 and GST-con80 have been described previously (McNally et al., 2000). A baculovirus encoding a 6-his fusion to enhanced green fluorescent protein (GFP) fused to a K255A mutant human p60 was constructed using the Bac to Bac System (Gibco-BRL Life Technologies). All proteins were expressed in Sf-9 cells and purified by nickel-chelate chromatography as described (Hartman et al., 1998; McNally et al., 2000).

ATPase assays

200 μl reactions containing 0.075 μM 6-his-wt-p60, varying concentrations of GFP-P loop K-A p60 and 1.3 mM ATP were incubated at 25°C. At eight 1 minute intervals, 25 μl aliquots were removed and analyzed for phosphate content by the malachite green method (Kodama et al., 1986). Velocities were determined for each set of eight data points. Heat inactivated GFP-P loop K-A p60 was produced by heating for 5 minutes at 75°C.

In vitro microtubule-severing assays

In vitro microtubule severing assays were carried out as previously described (McNally, 1998; McNally and Vale, 1993). Taxol-stabilized, tetramethyl-rhodamine-labeled microtubules were bound to the surfaces of a flow cell that was coated with a G234A mutant of human kinesin. Final concentration of polymerized tubulin in the reactions was determined to be 0.02 μM from the total length of surface-bound microtubules. Reactions were initiated by perfusing microtubules with a solution of 0.1 μM 6-his-human p60 + GST-con80 and varying concentrations of GFP-P loop K-A p60 in 20 mM K-Hepes, 4 mM MgSO4, 0.2 mM EGTA, 1.8 mM ATP, 20 μM taxol, 100 μg/ml BSA, pH 7.5. Reactions were stopped after 4 minutes by perfusing microtubules with 0.1% glutaraldehyde in 80 mM K-Pipes, 1 mM $MgCl_2$, 1 mM EGTA, pH 6.8. The ratio of free p60 to tubulin cannot be determined from these values since analysis of integrated GFP-fluorescence on flow-cell surfaces indicated that there was 10-times more GFP-p60 bound to the glass surface than bound to microtubules.

Cell culture and transfections

CV-1 cells were grown in Optimem (Gibco-BRL Life Technologies) medium supplemented with 10% fetal bovine serum (FBS), penicillin and streptomycin. Cells were plated on coverslips before transfecting plasmid DNAs with Lipofectamine Plus (Gibco-BRL Life Technologies), always in the presence of 10% FBS. The yellow fluorescent protein (YFP)-tubulin integrated CV-1 cell line was generated by co-transfecting pEYFP-Tub (Clontech Laboratories) with pCMV-ouabain (Pharmingen) and selecting for integrated cell lines with 1 μM ouabain. All plasmids encoding katanin fragments or mutants were constructed in the vectors pEGFP-C1, pECFP-C1 or pdsRed2-C1 (Clontech Laboratories).

Chariot-based protein transfection

To introduce anti-p60 IgG into CV-1 cells, cells were grown on 25 mm round coverslips in 30 mm dishes. A mixture of 18 μl Chariot reagent (Active Motif; Carlsbad, CA) and 36 μg IgG in serum-free Optimem were added to cells for 2 hours. Media was then replaced with Optimem containing 10% FBS and cells were fixed 2 hours later. Cells containing cytoplasmic IgG were identified by staining with anti-rabbit IgG secondary antibody.

Two different regimes were used to ensure that cells were in their first mitosis after transfection. In one regime, CV-1 cells were arrested at G1-S with 2 mM thymidine, transfected, released into thymidine-free medium and fixed 12 hours after release. In the second regime, unsynchronized CV-1 cells were fixed 12-20 hours after transfection.

Determination of γ-tubulin areas at spindle poles

Fixation

Cells growing on coverslips were fixed by removing culture medium and adding 3.7% formaldehyde (v/v), 0.25% glutaraldehyde (v/v), 80 mM Pipes, pH 6.8, 100 mM NaCl, 1 mM $MgCl_2$, 5 mM EGTA, 0.2% Triton X-100 (v/v) for 10-15 minutes at 25°C. Coverslips were post-fixed in 100% methanol at –20°C. Prior to immunostaining, coverslips were treated with 100 mM $NaBH_4$ in 50 mM Tris, pH 10.3, 100 mM NaCl, for 5-10 minutes, 25°C, to reduce any remaining aldehydes.

γ-tubulin immunostaining

Coverslips were immunostained sequentially with a 1:1000 dilution of GTU-88 anti-γ-tubulin monoclonal antibody (Sigma) and a 1:1000 dilution of Alexa Fluor 594 goat anti-mouse IgG (Molecular Probes) with DAPI and then mounted in Mowiol mounting medium (Calbiochem) including 2.5% (w/v) 1,4-diazobicyclo[2.2.2]-octane. Cells were never double-labeled with anti-α-tubulin when γ-tubulin areas were determined. Cell cycle stage was determined from DAPI staining. All cells without a nuclear envelope and with condensed chromosomes that were not perfectly organized into a metaphase plate or into two sets of anaphase chromosomes were classified as ‘prometaphase’.

Quantitation of γ-tubulin staining areas

Cells expressing each transfected construct were identified by their GFP fluorescence and their mitotic stage determined by the organization of their DAPI-stained chromosomes. Centrosomes and spindle poles were identified by their intensely fluorescent, spherical areas of γ-tubulin staining. Each pole (or centrosome) was brought to sharpest focus, and the image recorded with a Nikon Microphot SA microscope with a 60× PlanApo 1.4 objective and a Quantix KAF 1400 CCD camera (Photometrics). Identical exposure times and gain settings were used to capture the images for all treatments.

To quantitate γ-tubulin staining areas, regions of cells with cytoplasmic levels of fluorescence intensity were selected manually. The average fluorescence intensity of a cytoplasmic region was

multiplied by a factor of 1.11 to yield a threshold fluorescence intensity. IP Lab Spectrum (Scanalytics) was used to identify all image pixels with fluorescence intensities greater than the threshold value and then to calculate the total area of the selected pixels at and around each spindle pole.

Estimation of cytoplasmic concentration of dominant negative katanin subunits

To establish a relationship between CFP fluorescence intensity and the molar concentration of CFP-P loop K-A p60, transfected cells were fixed and processed for immunofluorescence with anti-p60 antibodies. The over-expression level of p60 was estimated in several dozen transfected cells by determining the ratio of anti-p60 staining intensity in each transfected cell to that of an untransfected cell in the same field. The range of CFP fluorescence intensity in cells analyzed in Figs 5 and 6 correspond to concentrations 10-50-times greater than that of endogenous p60.

Nocodazole disassembly assay

CV-1 cells with the integrated YFP-tubulin construct were transfected on 25 mm coverslips. 12-20 hours post transfection, coverslips were assembled into perfusion chambers maintained at 37°C. Cells were imaged with the same system used for immunofluorescence. Mitotic CFP-expressing cells were identified quickly using reduced illumination. A single CFP fluorescence image was captured using fixed neutral density filters, exposure and gain so that the expression level could be estimated. 50 μl of culture medium containing 80 μM nocodazole was then added gently to the edge of the perfusion chamber and shuttered, time lapse acquisition of YFP fluorescence images was initiated. Diffusion of nocodazole to the imaged cell did not appear to be rate limiting as the fastest changes in YFP fluorescence intensity and spindle length always occurred in the first 5 seconds of the image sequence.

To analyze the rate of reduction in YFP fluorescence intensity in the spindle, pixels corresponding to each half spindle as well as a cytoplasmic region adjacent to the spindle were highlighted manually. The average pixel values of each of these three regions were determined and the ratio of each half spindle's average pixel value/the average cytoplasmic pixel value was determined for each frame. In control experiments on untreated cells, this ratio remained constant in time lapse sequences, whereas absolute pixel values decreased due to photobleaching. For nocodazole-treated cells, the ratio reached 1.0 when the spindle was no longer visible to the eye (when cytoplasmic and spindle fluorescence were equal). To allow comparison of spindle disassembly rates between cells with different starting ratios, the ratios were converted to a fractional scale where the starting ratio was defined as 100% (of starting ratio) and the ratio at spindle disappearance was defined as 0% (of starting ratio).

Fluorescence recovery after photobleaching

FRAP experiments were carried out on a Zeiss 410 laser scanning confocal microscope using a krypton/argon laser and the 'activate' software for bleaching of YFP-tubulin. Cells were transiently transfected with dsRed2 fusion proteins.

Results

A P loop K-A substitution mutant of human p60 is a specific inhibitor of wild-type katanin in vitro and in vivo

The study of katanin's function in mammalian cells requires specific inhibitors that affect katanin's activity without directly affecting microtubules or other proteins. A single amino acid substitution of the P loop lysine for alanine (P loop K-A) in VPS4, an AAA enzyme closely related to katanin, generates a dominant inhibitor of the ATPase activity of wild-type VPS4 protein (Babst et al., 1998). Structural studies of other AAA enzymes (Lenzen et al., 1998; Yu et al., 1998; Zhang et al., 2000) suggest that the P loop K-A mutant of VPS4 may act by interfering with the oligomerization of wild-type VPS4 subunits. To test whether a similar mutation in the AAA katanin subunit (p60) would generate a dominant inhibitor of wild-type katanin, the ATPase activity of wild-type p60 was monitored in the presence of GFP-P loop K-A p60 and in the absence of microtubules. As show in Table 1, GFP-P loop K-A p60 reduced the ATPase activity of wild-type p60 in a concentration-dependent manner. Heat denatured GFP-P loop K-A p60 did not affect the ATPase velocity of wild-type katanin, indicating that this inhibition requires properly folded protein. These data indicate that GFP-P loop K-A p60 can inhibit wild-type p60 in vitro by interfering directly with the ATPase cycle of wild-type p60.

Table 1. Inhibition of wild-type katanin's basal ATPase activity by GFP-P loop K-A p60

Ratio of wt-p60:GFP-P loop K-A p60	ATPase ($\mu M\ PO_4$/minute/μM p60)
1:0	1.25
	1.12
1:4	0.70
	0.74
1:6	0.33
	0.33
1:4 (denatured GFP-P loop K-A p60)	1.17
	1.11
1:6 (denatured GFP-P loop K-A p60)	1.09

Results from two independent experiments are shown.

To determine whether the effect of GFP-P loop K-A p60 on wild-type p60 was sufficient to prevent microtubule severing in vitro, taxol-stabilized microtubules were incubated in the presence of purified recombinant wild-type and P loop K-A human p60 katanin. Purified wild-type human p60 pre-associated with GST-con80 (a GST fusion to the C-terminal domain of p80 katanin) mediated complete disassembly of microtubules (Fig. 1; Table 2) as previously reported (McNally et al., 2000). Inclusion of a fourfold molar excess of a purified GFP fusion to P loop K-A human p60 resulted in complete inhibition of microtubule disassembly by wild-type p60 (Fig. 1; Table 2). Heat-denatured GFP-P loop K-A p60 failed to inhibit the microtubule disassembly activity of wild-type p60. Because the con80 domain of p80 katanin binds to and activates the p60 subunit (McNally et al., 2000), it is possible that GFP-P loop K-A p60 acts by sequestering GST-con80 away from the wild-type p60 subunits. In this scenario, addition of excess GST-con80 should alleviate the inhibition caused by P loop K-A p60. GFP-P loop K-A p60 was pre-incubated with a slight excess of GST-con80 and tested for inhibition of wild-type p60. As shown in Table 2, GFP-P loop K-A p60/GST-con80 inhibits wild-type p60 as well as GFP-P loop K-A p60 alone, indicating that sequestering the con80 domain is not the mechanism of inhibition. A GFP fusion to a double mutant p60 (GFP-ΔN-P loop K-A p60), bearing the P loop K-A substitution as well as a deletion of the N-terminal

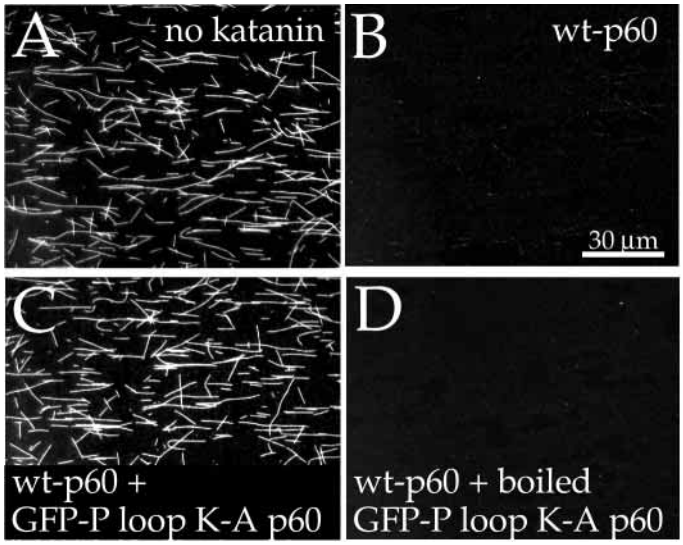

Fig. 1. GFP-P loop K-A p60 inhibits the in vitro microtubule-severing activity of wild-type p60. Fluorescence images were captured after taxol-stabilized, tetra-methyl rhodamine labeled microtubules were perfused with different protein solutions containing Mg^{2+}-ATP, incubated for 4 minutes, then fixed with glutaraldehyde. (A) No katanin. (B) 0.1 μM 6his-wt-p60 pre-bound with 0.1 μM GST-con80. (C) 0.1 μM 6his-wt-p60 pre-bound with 0.1 μM GST-con80 + 0.4 μM GFP-P loop K-A p60. (D) 0.1 μM 6his-wt-p60 pre-bound with 0.1 μM GST-con80 + 0.4 μM heat-inactivated GFP-P loop K-A p60.

Table 2. In vitro inhibition of wild-type human p60 katanin

Proteins in reaction	Molar ratio of wt:mutant p60	MT-severing activity*
No katanin	0:0	–
P loop K-A p60/GST-con80	0:1	–
wt-p60/GST-con80	1:0	+++
wt-p60/GST-con80+P loop K-A p60	1:1	+++
wt-p60/GST-con80+P loop K-A p60	1:2	+
wt-p60/GST-con80+P loop K-A p60	1:4	–
wt-p60/GST-con80+P loop K-A/GST-con80	1:4	–
wt-p60/GST-con80+boiled P loop K-A p60	1:4	+++
wt-p60/GST-con80+ΔN-P loop K-A p60	1:4	+++

Severing reactions contained 0.02 μM polymerized tubulin and 0.1 μM 6his-p60/GST-con80. P loop K-A p60/GST-con80 was added at ratios of 1:1, 1:2 etc to 6his-p60. Total GFP-p60 fluorescence associated with the coverslips was ten times that associated with the microtubules (MT).

*–Average MT length=15 μm; +++, MT gone; +, MT average length reduced by 2 μm.

29 amino acids previously shown to be required for association with con80 (McNally et al., 2000), did not inhibit wild-type p60 at concentrations effective for P loop K-A p60 (Table 2). This result demonstrates that GFP-ΔN-P loop K-A provides an appropriate negative control for katanin inhibition studies.

If GFP-P loop K-A p60 is to be useful as a specific in vivo inhibitor of wild-type katanin, it must inhibit the endogenous wild-type p60 without binding to microtubules. To test whether GFP-P loop K-A p60 can inhibit wild-type p60 in vivo and whether microtubule binding occurs in vivo, we analyzed the activities and localization of katanin subunits expressed in HeLa cells and CV-1 cells by transient transfection. When HeLa cells were co-transfected with an epitope-tagged wild-type p60 and GFP, a high percentage (54±8%, *n*=552 cells, 4 transfections) of the GFP-positive cells exhibited extensive microtubule disassembly revealed by a 2-10-fold reduction in the intensity of anti-α-tubulin immunofluorescence staining as previously reported (McNally et al., 2000). By contrast, co-transfection of GFP-P loop K-A p60 with wild-type p60 resulted in more than a 50-fold reduction in the fraction of co-transfected cells exhibiting microtubule disassembly (0.7±0.55%, *n*=1272 cells, 3 transfections). This result indicates that GFP-P loop K-A p60 is a potent inhibitor of wild-type p60 in vivo.

If in vivo inhibition of wild-type katanin by GFP-P loop K-A p60 is due to competition for microtubule binding sites, then GFP- P loop K-A p60 should exhibit some steady state localization to microtubules in vivo. To determine whether dominant-negative katanin proteins bind to microtubules in vivo, we examined their subcellular localization in transfected CV-1 cells. In interphase CV-1 cells, neither CFP-P loop K-A p60 nor CFP-con80 showed any co-localization with microtubules. This result indicates that in vivo inhibition of wild-type katanin by GFP-P loop K-A p60 most likely occurs by direct interaction with wild-type katanin subunits rather than by competing for microtubule binding sites. Surprisingly, CFP-ΔN-P loop K-A frequently did show co-localization with interphase microtubules. This result indicated that any non-specific effects due to microtubule binding in vivo should be more severe for CFP-ΔN-P loop K-A than for CFP-P loop K-A p60. In mitotic CV-1 cells expressing very low levels of CFP fusion protein, CFP-P loop K-A p60 and CFP-con80 localized in large spindle pole structures, just like endogenous p60 katanin (McNally and Thomas, 1998). By contrast, CFP-ΔN-P loop K-A p60 never exhibited localization in large spindle pole structures. The spindle pole localization of CFP-P loop K-A p60 and CFP-con80 in mitotic CV-1 cells indicated that these fusion proteins should be able to access the endogenous katanin in mitotic spindle poles.

Katanin's activity is not required for spindle assembly, anaphase or cytokinesis

To test whether inhibition of katanin with CFP-P loop K-A p60 would prevent spindle assembly or function, CV-1 cells with an integrated YFP-α-tubulin construct were transiently transfected with CFP or CFP-P loop K-A p60. Mitotic spindles were monitored by time lapse imaging of YFP-tubulin fluorescence. Six out of six CFP-transfected cells that were initially observed with a mono-astral array of microtubules assembled a bipolar spindle of metaphase length (9-12 μm) in 9-24 minutes. Likewise, four of five CFP-P loop K-A-transfected cells that were initially observed with a mono-astral array of microtubules assembled a bipolar spindle of metaphase length in 10-21 minutes. Only one out of five CFP-P loop K-A-transfected cells failed to assemble a bipolar spindle of metaphase length before filming was stopped at 244 minutes. Thus, the majority of CFP-P loop K-A-transfected cells are able to assemble a bipolar spindle with normal kinetics.

If katanin inhibition causes a change in the occupancy or tension of microtubules at kinetochores, a delay in the

Table 3. Increase in γ-tubulin area during the cell cycle of CV-1 cells

Cell cycle stage	Interphase	Prophase	Prometaphase	Metaphase	Anaphase
γ-Tubulin area (μm^2)	0.48±0.12 (*n*=16)	1.08±0.28 (*n*=42)	4.4±2.8 (*n*=104)	10±4.4 (*n*=20)	6.0±4.4 (*n*=76)

metaphase-anaphase transition would be expected (Rudner and Murray, 1996). Thirteen out of fourteen CFP-transfected cells initially observed with metaphase length bipolar spindles completed anaphase and cytokinesis in 17-22 minutes. These cells spent 2-58 minutes with a metaphase length spindle before initiating anaphase. One CFP-transfected cell completed anaphase after spending 199 minutes with a metaphase length spindle and one failed to enter anaphase after 189 minutes of filming. Nine out of thirteen CFP-P loop K-A transfected cells initially observed with metaphase length spindles completed anaphase and cytokinesis in 10-30 minutes. The majority of these cells (8/9) spent 22-105 minutes with a metaphase length spindle. One cell spent 244 minutes with a metaphase length spindle before completing normal anaphase and cytokinesis. A minority (3/13) of CFP-P loop K-A-transfected cells spent 287-317 minutes with a metaphase length spindle before filming was stopped. These results indicate that the majority of CFP-P loop K-A-transfected cells did not exhibit a delay in the metaphase-anaphase transition and exhibited normal anaphase and cytokinesis.

The area occupied by γ-tubulin at prometaphase spindle poles is dependent on microtubules

To test the hypothesis that recapping of microtubule ends generated by katanin-mediated severing is partly responsible for the broad distribution of γ-tubulin during mitosis (Lajoie-Mazenc et al., 1994), we first devised an objective assay for the area occupied by γ-tubulin in the spindle. CV-1 cells were fixed and stained with anti-γ-tubulin monoclonal antibody and fluorescent secondary antibody. For each cell, the average pixel value of anti-γ-tubulin staining in the cytoplasm was determined. The area occupied by pixels with a value greater than 1.11 times the cytoplasmic value was determined as described in Materials and Methods. As shown in Table 3, the area occupied by γ-tubulin increases dramatically at the interphase-prophase transition and again at the prophase-prometaphase transition. If this increase in γ-tubulin area during M phase is really an indirect consequence of the generation of microtubule minus ends, then this increase in area should be sensitive to microtubule depolymerization with nocodazole. CV-1 cells were treated with 20 μM nocodazole for either 30 minutes or 12 hours. Most mitotic cells in the 30 minute treatment are likely to have entered M phase before microtubule depolymerization whereas most mitotic cells in the 12 hour treatment are likely to have entered M phase without microtubules. (Both treatments allow complete microtubule disassembly in mitotic CV-1 cells as assayed by anti-α-tubulin immunofluorescence.) As shown in Table 4, nocodazole treatment had no effect on γ-tubulin areas at interphase centrosomes but reduced γ-tubulin areas in prophase and prometaphase cells close to those values observed in interphase. The histogram analysis in Fig. 2 shows the sensitivity of prometaphase γ-tubulin area to a 30 minute nocodazole treatment and illustrates the variability of this area in control cells. These results are consistent with two models explaining the increased γ-tubulin area observed in mitotic CV-1 cells, association of γ-TuRCs with dynein complexes on the sides of microtubules (Young et al., 2000) or the presence of microtubule minus ends distributed throughout the spindle.

The area occupied by γ-tubulin at prometaphase spindle poles is dependent on katanin's activity and spindle pole localization

To test whether the increase in area occupied by γ-tubulin in mitosis is dependent on katanin-mediated microtubule severing, γ-tubulin areas were determined in CV-1 cells expressing GFP-P loop K-A p60 due to transient transfection. As shown in the histogram in Fig. 3C, nearly 40% of cells in their first prometaphase after expression of the dominant katanin inhibitor exhibited interphase-like γ-tubulin areas (<1.6 μm^2) compared with only 5% of control GFP-expressing cells. Because 60% of prometaphase GFP-P loop K-A-expressing cells had normal γ-tubulin areas, simple comparison of average values was not informative. However, analysis of these data sets using the

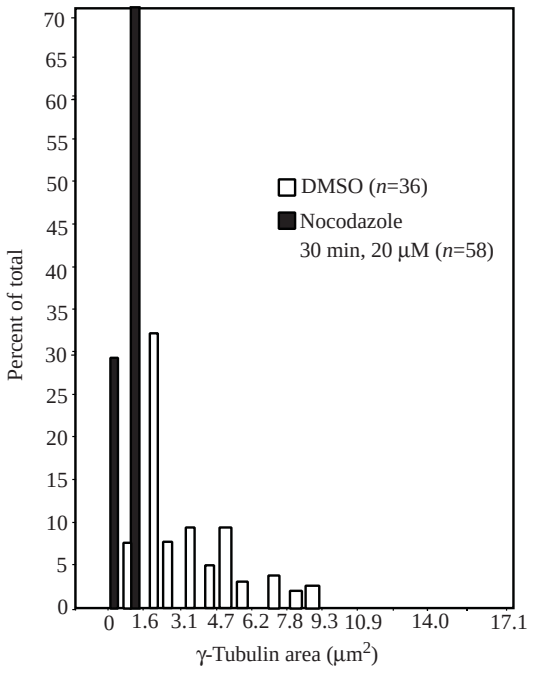

Fig. 2. The area occupied by γ-tubulin at prometaphase spindle poles is dependent on polymerized microtubules. CV-1 cells were treated for 30 minutes with either nocodazole added as a stock solution dissolved in DMSO (20 μM nocodazole, 0.1% DMSO final concentration) or with 0.1% DMSO only. Cells were fixed and stained with an anti-γ-tubulin monoclonal antibody. Prometaphase cells were identified by morphology of DAPI-stained chromosomes and the area of increased γ-tubulin staining intensity was determined as described in Materials and Methods. The histogram shows the fraction of cells with γ-tubulin areas falling within each range of values shown.

Table 4. Nocodazole sensitivity of γ-tubulin areas in CV-1 cells

Cell cycle stage	Interphase			Prophase			Prometaphase/pseudo-prometaphase		
Treatment	DMSO	Nocodazole (30 min)	Nocodazole (12 h)	DMSO	Nocodazole (30 min)	Nocodazole (12 h)	DMSO	Nocodazole (30 min)	Nocodazole (12 h)
γ-Tubulin area (μm^2)	0.48±0.14 (*n*=34)	0.48±0.11 (*n*=20)	0.52±0.096 (*n*=49)	1.44±0.56 (*n*=52)	0.68±0.28 (*n*=36)	0.52±0.14 (*n*=58)	3.4±2.4 (*n*=62)	0.92±0.18 (*n*=69)	0.64±0.14 (*n*=67)

Nocodazole was added to the culture medium from a stock solution dissolved in DMSO. Final concentrations were 20 μM nocodazole, 0.1% DMSO. Control cultures were treated with only 0.1% DMSO.

Mann-Whitney nonparametric test revealed that the difference between GFP-expressing and GFP-P loop K-A p60-expressing cells was highly significant (*P*=0.0001). Prolonged (48 hour) expression of GFP-P loop K-A p60 resulted in a more severe reduction in γ-tubulin areas with many prometaphase cells exhibiting no detectable foci of γ-tubulin staining (D.B. and F.J.M., unpublished). The apparent loss of γ-tubulin foci in some cells may indicate a physiological response to long term expression of this particular fusion protein or that our imaging system is not adequate to distinguish very small, dim foci from bright cytoplasmic staining. Expression of GFP-ΔN-P loop K-A p60, which was a poor inhibitor of katanin in vitro, did not cause a significant reduction in prometaphase γ-tubulin areas (Fig. 3D). To further verify that the reduced γ-tubulin areas in prometaphase cells were due to inhibition of katanin, a previously described anti-human p60 katanin antibody that inhibits microtubule severing in *Xenopus* extracts (McNally and Thomas, 1998) was introduced into CV-1 cells using a viral fusion peptide (see Materials and Methods). Cells were treated with either anti-p60 antibody or a control IgG isolated from the same serum but affinity depleted of anti-p60 antibodies; cells were fixed 4 hours after initially adding antibodies. Anti-rabbit IgG immunofluorescence confirmed that the anti-p60 antibody but not the control antibody localized to mitotic spindle poles (D.B. and F.J.M., unpublished). Analysis of prometaphase γ-tubulin areas in anti-p60 containing cells compared with control IgG-containing cells revealed a significant (*P*=0.02) reduction due to katanin inhibition (Fig. 3E). Inhibition of katanin did not have a statistically significant effect on γ-tubulin areas in

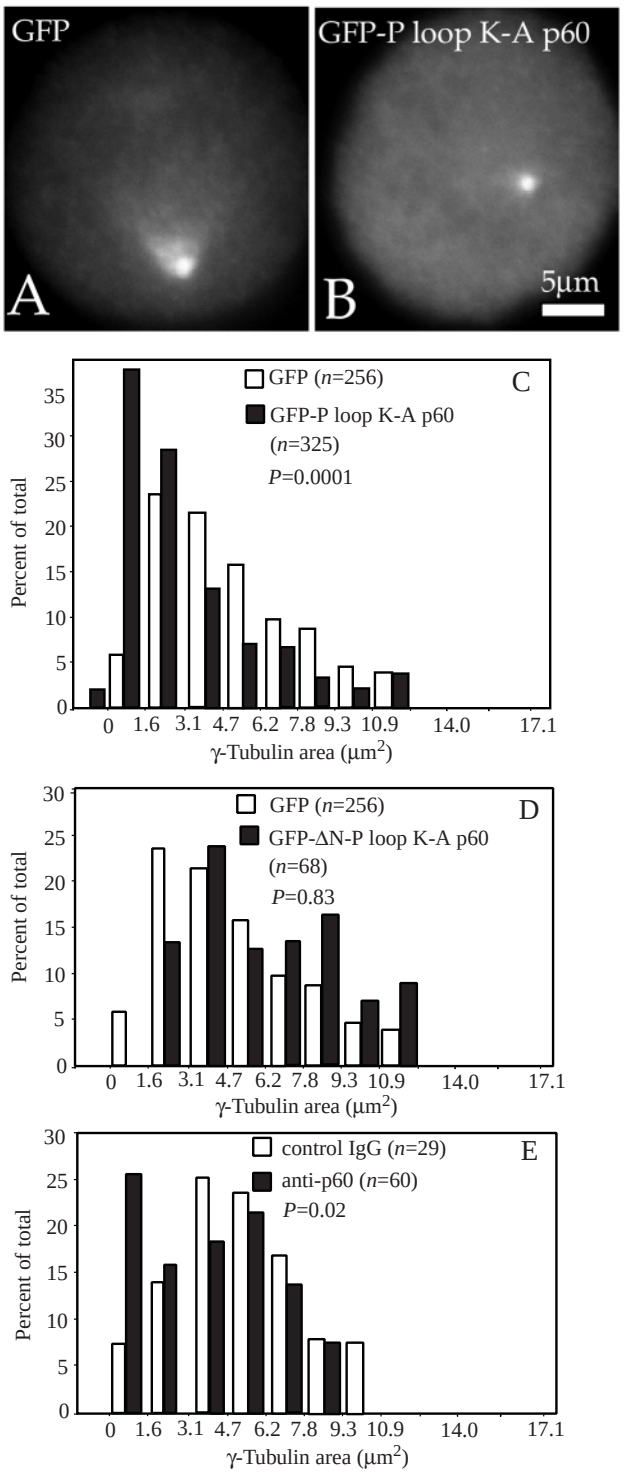

Fig. 3. Katanin inhibition reduces the area occupied by γ-tubulin at prometaphase spindle poles. (A-D) CV-1 cells were transfected with plasmids encoding GFP fusions to the dominant katanin inhibitor, P loop K-A p60, the weak katanin inhibitor, ΔN-P loop K-A p60, or GFP alone. Cells were fixed and stained with an anti-γ-tubulin monoclonal antibody within 24 hours of transfection or within 12 hours of release from a thymidine block to ensure that mitotic cells were in their first mitosis after expression of the GFP-fusion. The fluorescence micrographs show anti-γ-tubulin staining of representative prometaphase cells expressing GFP (A) or GFP-P loop K-A p60 (B). The histograms in C-E show the fraction of prometaphase cells with γ-tubulin areas falling within each range of values shown. *P* indicates the significance of the difference between control (GFP alone) and experimental populations as determined with the Mann-Whitney test. (E) Affinity-purified anti-p60 katanin antibodies or a control IgG were introduced into CV-1 cells by Chariot mediated protein transfection (see Materials and Methods). Cells were fixed 4 hours after initiation of the antibody treatment and prometaphase cells containing significant cytoplasmic IgG concentrations were identified by DAPI-stained chromosome morphology and anti-rabbit IgG staining. Areas of increased γ-tubulin staining intensity were analyzed as in C and D.

interphase, metaphase or anaphase cells relative to cells expressing GFP alone (D.B. and F.J.M., unpublished; see Discussion). The observed reduction of γ-tubulin areas by inhibition of a microtubule-severing protein is consistent with the model in which the broad distribution of γ-tubulin in spindles is at least partly due to the presence of microtubule minus ends.

To test the importance of katanin's localization at spindle poles, we analyzed the effects of a GFP fusion to the C-terminal con80 domain of human p80 katanin. Over-expression of this domain of p80 causes the mislocalization of endogenous p60 from mitotic spindle poles but does not inhibit microtubule severing activity of wild-type p60 (McNally et al., 2000). Analysis of prometaphase γ-tubulin areas in GFP-con80-expressing CV-1 cells 12-20 hours after transfection revealed no significant decrease relative to GFP expressing cells (P=0.18) as indicated in Fig. 4A. However, analysis of γ-tubulin areas 48 hours post-transfection (Fig. 4B) revealed that GFP-con80 did cause a significant reduction in prometaphase γ-tubulin areas relative to GFP expressing cells (P=0.0067) after prolonged expression. Thus, eliminating the local concentration of katanin at spindle poles has the same effect as inhibiting katanin's severing activity, although with slower kinetics.

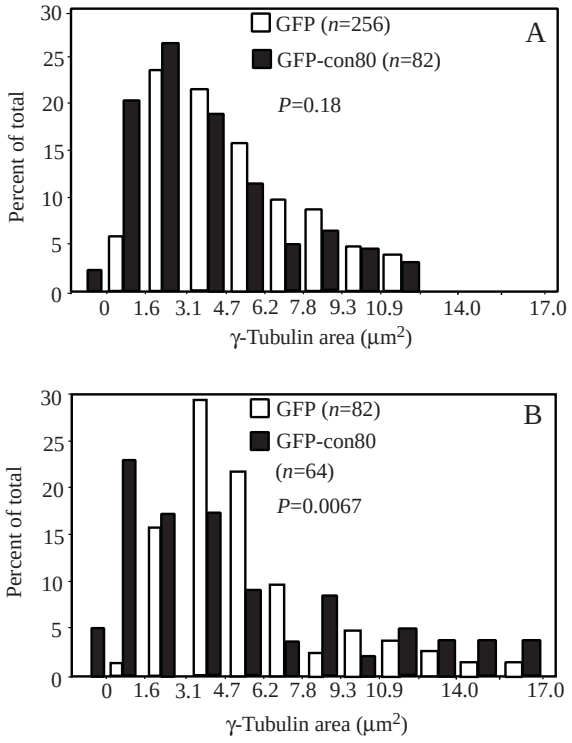

Fig. 4. Prolonged mislocalization of katanin from spindle poles results in a reduction of the γ-tubulin focus at prometaphase spindle poles. (A,B). CV-1 cells were transfected with plasmids encoding a GFP fusion to the C-terminal, con80, domain of p80 katanin, which causes endogenous p60 to mislocalize from spindle poles to the cytoplasm, or GFP alone. Cells were fixed and stained with an anti-γ-tubulin monoclonal antibody either 20 hours (A) or 48 hours (B) post-transfection. The histogram shows the fraction of cells with γ-tubulin areas falling within each range of values shown. *P* indicates the significance of the difference between control (GFP alone) and experimental populations as determined with the Mann-Whitney test.

The reduction in γ-tubulin areas by katanin inhibition was not accompanied by gross abnormalities in spindle structure. Analysis of GFP-P loop K-A p60-expressing cells by anti-α-tubulin staining and anti-NuMA staining revealed that these spindles exhibited a normal morphology (D.B. and F.J.M., unpublished). One trivial explanation for the extreme reduction in γ-tubulin area might be that targeting of GFP-P loop p60 to centrosomes causes the degeneration of centrioles as has been observed in cells microinjected with anti-glutamylated tubulin antibodies (Bobinnec et al., 1998). To test this possibility, GFP-P loop K-A p60 expressing cells were fixed 48 hours post-transfection and stained with anti-centrin antibody. Normal centriole staining was observed in prometaphase cells (D.B. and F.J.M., unpublished), indicating that the reduction in γ-tubulin area is not due to centriole degeneration. Thus katanin inhibition appears to have a specific effect on γ-tubulin distribution in prometaphase spindles.

The rate of spindle disassembly in nocodazole is dependent on katanin's activity and katanin's localization at spindle poles

Because microtubules polymerize and depolymerize from their ends, a spindle with an increased number of plus and minus ends due to katanin-mediated severing should disassemble faster when polymerization is blocked with nocodazole. To test this hypothesis, we monitored the microtubule disassembly rate in mitotic CV-1 cells expressing an integrated YFP-tubulin construct and transiently transfected CFP fusion proteins. The rate of microtubule disassembly was determined by monitoring the rate of decrease in YFP-tubulin fluorescence intensity by

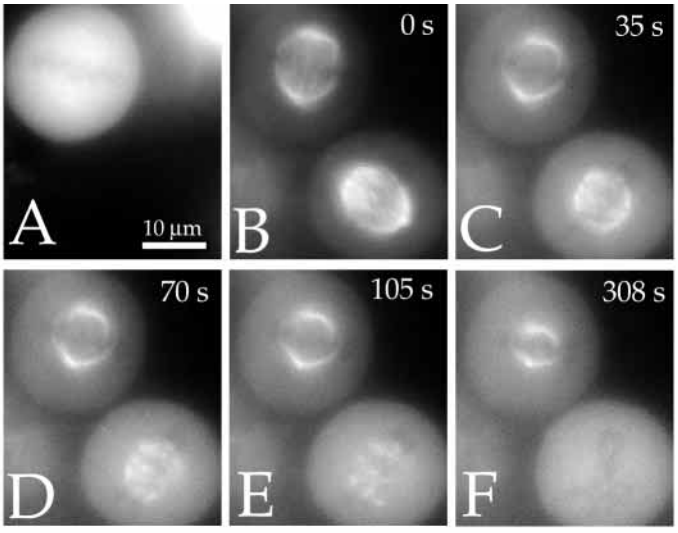

Fig. 5. Inhibition of katanin by CFP-P loop K-A p60 reduces the rate of nocodazole-mediated spindle disassembly. CV-1 cells with an integrated YFP-α-tubulin transgene were transiently transfected with CFP-P loop K-A p60 and mounted in a perfusion chamber. Transfected cells were identified by CFP fluorescence (A) and spindle disassembly was monitored by shuttered, time-lapse imaging of YFP-fluorescence (B-F) after perfusion with nocodazole. Note that the spindle in the untransfected cell (bottom right) shortened and disappeared rapidly, whereas the spindle in the CFP-P loop K-A p60-expressing cell (top left) shortened and faded much more slowly.

time-lapse imaging of living cells perfused with high concentrations of nocodazole (estimated 20 μM final concentration; see Materials and Methods). As shown in Fig. 5, control spindles perfused with nocodazole shortened to about half their starting length before the fluorescence intensity of YFP-tubulin in the spindle decreased to background levels. A plot of YFP-tubulin fluorescence intensity decrease over time reveals a rapid rate of spindle disassembly in control cells (Fig. 6A). Cells in which katanin was inhibited by CFP-P loop K-A p60 exhibited reduced rates of spindle disassembly, but spindles eventually disassembled completely. A large difference between control and CFP-P loop p60-expressing cells was observed in the time required to achieve 80% loss in YFP-tubulin fluorescence intensity (20% of initial intensity in Fig. 6A). Times required to achieve 80% loss of YFP-tubulin spindle intensity are displayed as histograms in Fig. 6B-F. In roughly 60% of cells in which katanin was inhibited (CFP-P loop K-A p60) or mislocalized from spindle poles (CFP-con80), the time to 80% loss of spindle intensity was much greater than is ever observed in control spindles. CFP-ΔN-P loop K-A p60, which was a poor inhibitor of severing and had no effect on γ-tubulin areas, had very little effect on the rate of spindle disassembly in nocodazole (Fig. 6F).

Tubulin turnover in the spindle is not grossly affected by katanin mislocalization

It is possible that increasing the number of microtubule plus and minus ends in prometaphase by microtubule-severing might contribute to the increased rate of turnover between polymerized and unpolymerized tubulin pools that is observed in mitotic cells (Saxton et al., 1984; Zhai et al., 1996). To test this hypothesis, we monitored the rate of YFP-tubulin fluorescence recovery after photobleaching (FRAP) in spindles of CV-1 cells transiently expressing either dsRed2 (*Discosoma* red fluorescent protein) or dsRed2-con80 (to displace katanin from spindle poles). One half spindle was completely photobleached and recovery of the bleached half spindle was monitored by time-lapse confocal microscopy. To compensate for photobleaching during the recovery period, recovery was expressed as a ratio of the intensity of the bleached half spindle to that of the unbleached half spindle. This ratio should reach a value of 1.0 when the bleached tubulin is completely replaced by unbleached YFP-tubulin. As shown in the examples in Fig. 7, fluorescence of the bleached half spindle typically plateaued at a ratio lower than 1. This could be due to the slow turnover reported for kinetochore microtubules (Zhai et al., 1995) or it could be because a fraction of spindle microtubules was

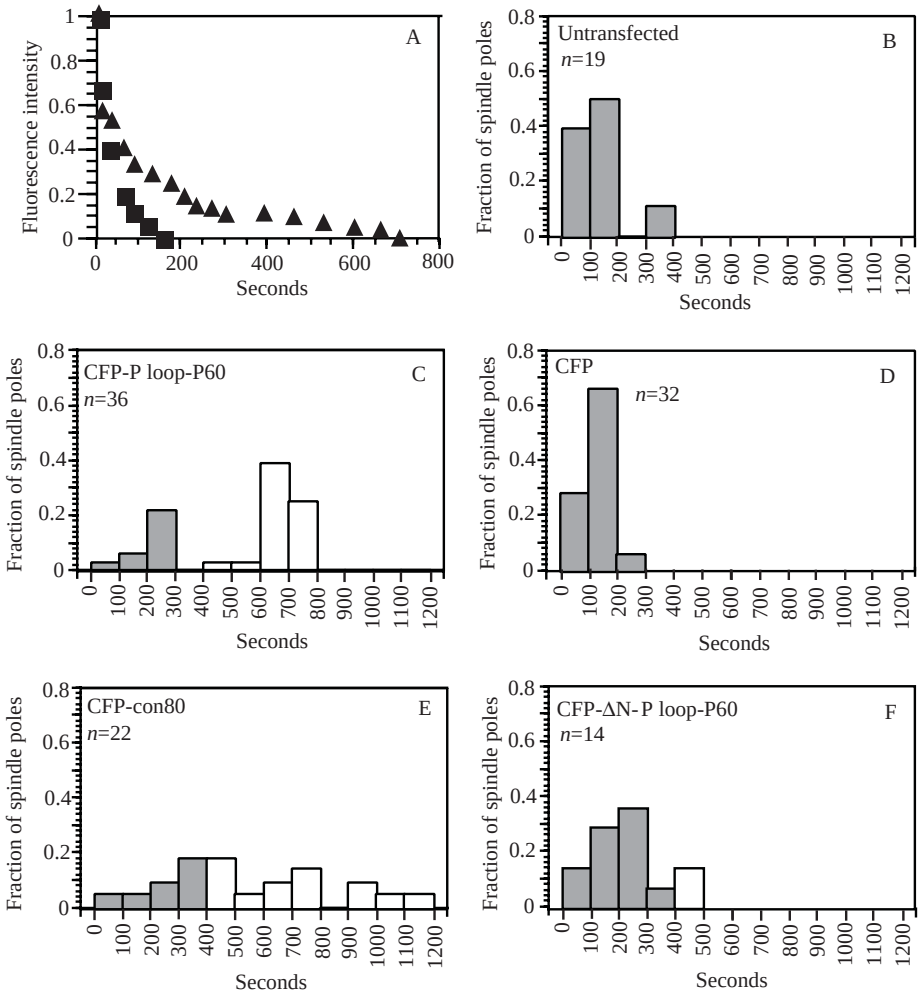

Fig. 6. Inhibition or mislocalization of katanin reduces the rate of nocodazole-mediated spindle disassembly. CV-1 cells with an integrated YFP-α-tubulin transgene were transiently transfected with different CFP-fusion constructs and mounted in a perfusion chamber. Transfected cells were identified by CFP fluorescence and spindle disassembly was monitored by shuttered, time-lapse imaging of YFP-fluorescence after perfusion with nocodazole. The ratio of spindle fluorescence/cytoplasmic fluorescence was determined for each frame of each YFP-time-lapse sequence and was normalized to a scale of 100% initial fluorescence ratio to 0% of initial fluorescence ratio as described in Materials and Methods. (A) Individual plots of decreasing YFP-fluorescence ratio over time in individual nocodazole-treated mitotic cells. ■, CFP; ▲, CFP-P loop K-A p60. To compare the effects of different CFP fusions on spindle disassembly rate, the time required to achieve 80% loss of normalized spindle intensity ratio (20% of initial ratio in A) was determined for each half spindle in each time lapse sequence. The number of half spindles exhibiting different ranges of time to 80% loss of spindle intensity ratio are displayed as histograms in B-F. Note that cells expressing CFP or CFP-ΔN-P loop K-A p60 exhibited disassembly times similar to those of untransfected cells (B,D,F). By contrast, 60-65% of cells expressing CFP-P loop K-A p60 or CFP-con80 exhibited spindle disassembly times slower than ever observed in untransfected or CFP-expressing cells (C,E). Grey bars indicate disassembly times observed in untransfected and CFP-transfected control cells. White bars indicate times slower than ever observed in control cells.

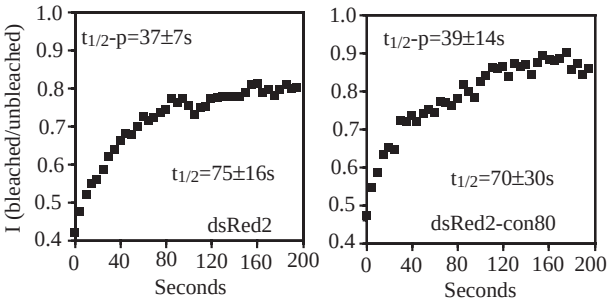

Fig. 7. Katanin mislocalization does not affect the rate of exchange between polymerized and unpolymerized tubulin as assayed by fluorescence recovery after photobleaching (FRAP). Mitotic CV-1 cells expressing an integrated YFP-tubulin gene and transiently expressing either dsRed2-con80, which mislocalizes endogenous katanin from spindle poles, or dsRed2 alone were located and subjected to FRAP analysis. One half spindle was completely photobleached with the krypton/argon laser of a laser scanning confocal microscope. Recovery of fluorescence due to incorporation of unbleached YFP-tubulin was monitored by time-lapse confocal microscopy. Examples of recovery by two individual spindles are shown. I(bleached/unbleached) is the ratio of fluorescence intensity of the bleached half spindle to that of the unbleached half spindle. $t_{½}$-p is the time to reach 50% recovery to the apparent plateau of recovery. $t_{½}$ is the predicted time to reach 50% recovery to an I(bleached/unbleached) ratio of 1. Averages with standard deviations were determined from 10 (dsRed2) or 13 (dsRed2-con80) spindles.

destroyed during photobleaching of the YFP. In these experiments, recovery could not be monitored for longer periods of time to distinguish between these possibilities. Cells expressing dsRed2-con80 or dsRed2 alone showed no differences in the half time to the plateau ratio, $t_{½}$-p, or in the predicted half time to a ratio of 1.0, $t_{½}$ (Fig. 7). There was also no difference in the degree of recovery at the observed plateau (dsRed2: 0.84±0.06 (n=10), dsRed2-con80: 0.87±0.09 (n=13)). Thus mislocalization of katanin from spindle poles did not have a discernable effect on tubulin turnover even though it slowed the rate of nocodazole-mediated spindle disassembly (Fig. 6E).

Discussion

In this study we have demonstrated that fusion proteins that inhibit (GFP-P loop K-A p60) or mislocalize (GFP-con80) endogenous katanin cause two phenotypes, a decrease in the area occupied by γ-tubulin in prometaphase and a decrease in the rate of nocodazole-mediated spindle disassembly. The fact that dispersal of katanin from the spindle pole has the same effect as inhibiting katanin's activity demonstrates that the increased concentration of katanin at mitotic spindle poles may be essential for its activity during mitosis.

The increase in γ-tubulin concentration and area of occupation during mitosis is probably due to multiple mechanisms. Khodjakov and Rieder concluded that the increase in γ-tubulin concentration at the centrosome did not require microtubules suggesting that an increased number of cytosolic γ-TuRCs can bind directly to the pericentriolar material during mitosis (Khodjakov and Rieder, 1999). Because their analysis was restricted to a region of interest (ROI) of fixed area, their conclusion does not bear directly on our analysis of γ-tubulin areas. In agreement with our results, Young et al. found that microtubules were involved in recruitment of γ-tubulin to mitotic centrosomes (Young et al., 2000). They also found (in agreement with our unpublished results) that dynein/dynactin is required for recruitment of γ-tubulin to the spindle. They concluded that γ-TuRC/pericentrin complexes were transported down the sides of microtubules by dynein/dynactin before docking in the pericentriolar material. Our finding that inhibition of microtubule severing causes a reduction in γ-tubulin areas at spindle poles strongly supports a model in which cytosolic γ-TuRCs cap new microtubule minus ends generated by severing. These new microtubules might be held in place in the spindle by the combined action of dynein/dynactin and NuMA (Merdes et al., 1996; Gaglio et al., 1997). Thus the effect of dynein inhibition is consistent with both models.

Multiple mechanisms behind the microtubule-dependent distribution of γ-tubulin may explain why katanin inhibition had a dramatic effect on the area occupied by γ-tubulin during prometaphase but had very little effect on metaphase or anaphase spindles. Kinetically slower mechanisms may be able to substitute for katanin by metaphase. Slower mechanisms for generating free microtubule minus ends around the centrosome might include other microtubule-severing proteins (Shiina et al., 1994) and transport of chromatin/GTP-Ran-induced microtubules to the spindle pole (Heald et al., 1997). Transport of γ-TuRC/pericentrin complexes down the sides of microtubules during metaphase (Young et al., 2000), even in the absence of uncapped microtubule minus ends, might also obscure the effects of katanin inhibition. Redundant mechanisms are also suggested by our finding that katanin inhibition only affects γ-tubulin areas in about half of prometaphase spindles, whereas nocodazole reduces γ-tubulin areas in nearly all spindles.

The finding that spindle microtubules disassemble more slowly in nocodazole when katanin is inhibited or mislocalized provides further support for a model in which katanin normally generates an increased number of microtubule ends in the spindle. Two 5 μm microtubules would be expected to depolymerize in half the time required for one 10 μm microtubule. However, the consequences of microtubule severing on steady state microtubule dynamics (without nocodazole) are less clear. Analysis of the exchange rate between polymerized and unpolymerized tubulin by FRAP revealed no gross differences between control cells and those in which katanin was mislocalized. Microtubule severing may have effects on tubulin turnover that are too subtle to be detected by FRAP; microtubule severing may not contribute to the rapid turnover of tubulin in mitotic cells or cells may compensate for a reduced number of microtubule ends by upregulating other proteins such as Kin I kinesins (Desai et al., 1999).

Severing of microtubules in the mitotic spindle could result in an increased number of non-centrosomal microtubules, uncapping of microtubule minus ends, an increase in microtubule number and a decrease in microtubule length. Because katanin is essential for *C. elegans* meiotic spindles, which are composed entirely of non-centrosomal microtubules (Srayko et al., 2000), it is unlikely that detachment of microtubules from the centrosome is the sole purpose of severing. If uncapping minus ends from γ-TuRCs is an

important function of severing, katanin inhibition may result in a reduction in the rate of poleward tubulin flux. Conversely, γ-tubulin inhibition might lead to an increase in the rate of flux. Poleward tubulin flux may be a minor component of anaphase A in PtK cells (Mitchison and Salmon, 1992) and a major component in *Xenopus* extract spindles (Desai et al., 1998). Our data are consistent with an increase in microtubule number due to severing in the mitotic spindle. Future work will focus on determining the functional importance of regulating microtubule number and length in mitotic and meiotic spindles.

We thank Jeff Salisbury for anti-centrin monoclonal antibody, Duane Compton for anti-NuMA antibodies and Trang Tran for generating the integrated YFP-tubulin cell line. This work was supported by GM53060 from the N.I.G.M.S.

References

Babst, M., Wendland, B., Estepa, E. J. and Emr, S. D. (1998). The VPS4 AAA ATPase regulates membrane association of a Vps protein complex required for normal endosome function. *EMBO J.* **17**, 2982-2993.

Belmont, L. D., Hyman, A. A., Sawin, K. E. and Mitchison, T. J. (1990). Real-time visualization of cell cycle-dependent changes in microtubule dynamics in cytoplasmic extracts. *Cell* **62**, 579-589.

Bobinnec, Y., Khodjakov, A., Mir, L. M., Rieder, C. L., Edde. B. and Bornens, M. (1998). Centriole disassembly in vivo and its effect on centrosome structure and function in vertebrate cells. *J. Cell Biol*. **143**, 1575-1589.

Carazo-Salas, R. E., Guarguaglini, G., Gruss, O. J., Segref, A., Karsenti, E. and Mattaj, I. W. (1999). Generation of GTP-bound Ran by RCC1 is required for chromatin-induced mitotic spindle formation. *Nature* **400**, 178-181.

Desai, A., Maddox, P. S., Mitchison, T. J. and Salmon, E. D. (1998). Anaphase A chromosome movement and poleward spindle microtubule flux occur at similar rates in *Xenopus* extract spindles. *J. Cell Biol*. **141**, 703-713.

Desai, A., Verma, S., Mitchison, T. J. and Walczak, C. E. (1999). Kin I kinesins are microtubule-destabilizing enzymes. *Cell* **96**, 69-78.

Gaglio, T., Dionne, M. A. and Compton, D. A. (1997). Mitotic spindle poles are organized by structural and motor proteins in addition to centrosomes. *J. Cell Biol*. **138**, 1055-1066.

Hartman, J. J., Mahr, J., McNally, K., Okawa, K., Iwamatsu, A., Thomas, S., Cheesman, S., Heuser, J., Vale, R. D. and McNally, F. J. (1998). Katanin, a microtubule severing protein, is a novel AAA ATPase that targets to the centrosome using a WD40-containing subunit. *Cell* **93**, 277-287.

Heald, R., Tournebize, R., Habermann, A., Karsenti, E. and Hyman, A. (1997). Spindle assembly in *Xenopus* egg extracts: respective roles of centrosomes and microtubule self-organization. *J. Cell Biol*. **138**, 615-628.

Keating, T. J. and Borisy, G. G. (2000). Immunostructural evidence for the template mechanism of microtubule nucleation. *Nat. Cell Biol*. **2**, 352-357.

Khodjakov, A. and Rieder, C. L. (1999). The sudden recruitment of γ-tubulin to the centrosome at the onset of mitosis and its dynamic exchange throughout the cell cycle, do not require microtubules. *J. Cell Biol*. **146**, 585-596.

Kodama, T., Fukui, K. and Kometani, K. (1986). The initial phosphate burst in ATP hydrolysis by myosin and subfragment-1 as studied by a modified malachite green method for determination of inorganic phosphate. *J. Biochem*. **99**, 1465-1472.

Lajoie-Mazenc, I., Tollon, Y., Detraves, C., Julian, M., Moisand, A., Gueth-Hallonet, C., Debec, A., Salles-Passador, I., Puget, A., Mazarguil, H. et al. (1994). Recruitment of antigenic gamma-tubulin during mitosis in animal cells: presence of gamma-tubulin in the mitotic spindle. *J. Cell Sci*. **107**, 2825-2837.

Lenzen, C. U., Steinmann, D., Whiteheart, S. W. and Weis, W. I. (1998). Crystal structure of the hexamerization domain of N-ethylmaleimide-sensitive fusion protein. *Cell* **94**, 525-536.

Mastronarde, D. N., McDonald, K. L., Ding, R. and McIntosh, J. R. (1993). Interpolar spindle microtubules in PTK cells. *J. Cell Biol*. **123**, 1475-1489.

McNally, F. J. (1998). Purification and assay of the microtubule-severing protein, katanin. *Methods Enzymol*. **298**, 206-218.

McNally, F. J. and Thomas, S. (1998). Katanin is responsible for the M-phase microtubule-severing activity in *Xenopus* eggs. *Mol. Biol. Cell* **9**, 1847-1861.

McNally, F. and Vale, R. (1993). Identification of katanin, an ATPase that severs and disassembles stable microtubules. *Cell* **75**, 419-429.

McNally, F. J., Okawa, K., Iwamatsu, A. and Vale, R. D. (1996). Katanin, the microtubule-severing ATPase, is concentrated at centrosomes. *J. Cell Sci*. **109**, 561-567.

McNally, K. P., Bazirgan, O. A. and McNally, F. J. (2000). Two domains of p80 katanin regulate microtubule severing and spindle pole targeting by p60 katanin. *J. Cell Sci*. **113**, 1623-1633.

Merdes, A., Ramyar, K., Vechio, J. D. and Cleveland, D. (1996). A complex of NuMA and cytoplasmic dynein is essential for mitotic spindle assembly. *Cell* **87**, 447-458.

Mitchison, T. (1989). Polewards microtubule flux in the mitotic spindle: evidence from photoactivation of fluorescence. *J. Cell Biol*. **109**, 637-652.

Mitchison, T. J. and Salmon, E. D. (1992). Poleward kinetochore fiber movement occurs during both metaphase and anaphase-A in newt lung cell mitosis. *J. Cell Biol*. **119**, 569-582.

Moritz, M., Zheng, Y., Alberts, B. M. and Oegema, K. (1998). Recruitment of the gamma-tubulin ring complex to *Drosophila* salt-stripped centrosome scaffolds. *J. Cell Biol*. **142**, 775-786.

Nachury, M. V., Maresca, T. J., Salmon, W. C., Waterman-Storer, C. M., Heald, R. and Weis, K. (2001). Importin-β is a mitotic target of the small GTPase Ran in spindle assembly. *Cell* **104**, 95-106.

Odde, D. J., Ma, L., Briggs, A. H., DeMarco, A. and Kirschner, M. W. (1999). Microtubule bending and breaking in living fibroblast cells. *J. Cell Sci*. **112**, 3283-3288.

Rodionov, V. I. and Borisy, G. G. (1997). Microtubule treadmilling in vivo. *Science* **275**, 215-218.

Rudner, A. D. and Murray, A. W. (1996). The spindle assembly checkpoint. *Curr. Opin. Cell Biol*. **8**, 773-780.

Rusan, N. M., Fagerstrom, C. J., Yvon, A. M. and Wadsworth, P. (2001). Cell cycle-dependent changes in microtubule dynamics in living cells expressing green fluorescent protein-α tubulin. *Mol. Biol. Cell* **12**, 971-980.

Saxton, W. M., Stemple, D. L., Leslie, R. J., Salmon, E. D., Zavortnik, M. and McIntosh, J. R. (1984). Tubulin dynamics in cultured mammalian cells. *J. Cell Biol*. **99**, 2175-2186.

Shiina, N., Gotoh, Y. and Nishida, E. (1994). Microtubule severing by elongation factor-1α. *Science* **266**, 282-285.

Srayko, M., Buster, D. W., Bazirgan, O. A., McNally, F. J. and Mains, P. E. (2000). MEI-1/MEI-2 katanin-like microtubule severing activity is required for *Caenorhabditis elegans* meiosis. *Genes Dev*. **14**, 1072-1084.

Waterman-Storer, C. M. and Salmon, E. D. (1997). Actomyosin-based retrograde flow of microtubules in the lamella of migrating epithelial cells influences microtubule dynamic instability and turnover and is associated with microtubule breakage and treadmilling. *J. Cell Biol*. **139**, 417-434.

Waters, J. C. and Salmon, E. (1997). Pathways of spindle assembly. *Curr. Opin. Cell Biol*. **9**, 37-43.

Wiese, C. and Zheng, Y. (2000). A new function for the γ-tubulin ring complex as a microtubule minus-end cap. *Nat. Cell Biol*. **2**, 358-364.

Wiese, C., Wilde, A., Moore, M. S., Adam, S. A., Merdes, A. and Zheng, Y. (2001). Role of importin-beta in coupling Ran to downstream targets in microtubule assembly. *Science* **291**, 653-656.

Wilde, A. and Zheng, Y. (1999). Stimulation of microtubule aster formation and spindle assembly by the small GTPase Ran. *Science* **284**, 1359-1362.

Young, A., Dictenberg, J. B., Purohit, A., Tuft, R. and Doxsey, S. J. (2000). Cytoplasmic dynein-mediated assembly of pericentrin and γ-tubulin onto centrosomes. *Mol. Biol. Cell* **11**, 2047-2056.

Yu, R. C., Hanson, P. I., Jahn, R. and Brunger, A. T. (1998). Structure of the ATP-dependent oligomerization domain of N-ethylmaleimide sensitive factor complexed with ATP. *Nat. Struct. Biol*. **5**, 803-811.

Zhai, Y., Kronebusch, P. J. and Borisy, G. G. (1995). Kinetochore microtubule dynamics and the metaphase-anaphase transition. *J. Cell Biol*. **131**, 721-734.

Zhai, Y., Kronebusch, P. J., Simon, P. M. and Borisy, G. G. (1996). Microtubule dynamics at the G2/M transition: abrupt breakdown of cytoplasmic microtubules at nuclear envelope breakdown and implications for spindle morphogenesis. *J. Cell Biol*. **135**, 201-214.

Zhang, X., Shaw, A., Bates, P. A., Newman, R. H., Gowen, B, Orlova, E., Gorman, M. A., Kondo, H., Dokurno, P., Lally, J. et al. (2000). Structure of the AAA ATPase p97. *Mol Cell*. **6**, 1473-1484.

Zheng, Y., Wong, M. L., Alberts, B. and Mitchison, T. (1995). Nucleation of microtubule assembly by a γ-tubulin-containing ring complex. *Nature* **378**, 578-583.